AFRL-SR-AR-TR-08-0286

REPORT DOCUMENTATION PAGE

1. REPORT DATE *(DD-MM-YYYY)*	2. REPORT TYPE	3. DATES COVERED *(From - To)*
31-03-2008	Final Performance Report	03-29-2004 to 31-12-2007

4. TITLE AND SUBTITLE
Combined High Temperature Aerothermal-Structural Physical Property Testing of Ceramic Matrix Composites

5a. CONTRACT NUMBER

5b. GRANT NUMBER
FA9550-05-1-0212

5c. PROGRAM ELEMENT NUMBER

6. AUTHOR(S)
D. E. King and D. G. Drewry

5d. PROJECT NUMBER

5e. TASK NUMBER
JHU/APL Task FG1KP

5f. WORK UNIT NUMBER

7. PERFORMING ORGANIZATION NAME(S) AND ADDRESS(ES)
The Johns Hopkins
University Applied Physics
Laboratory
11100 Johns Hopkins Road
Laurel, MD 20723-6099

8. PERFORMING ORGANIZATION REPORT

9. SPONSORING / MONITORING AGENCY NAME(S) AND ADDRESS(ES)
USAF, AFRL
AFOSR/NA
875 N. Randolph St., Rm. 3112
Arlington, VA 22203

10. SPONSOR/MONITOR'S ACRONYM(S)

11. SPONSOR/MONITOR'S REPORT NUMBER(S)

12. DISTRIBUTION / AVAILABILITY STATEMENT
Unlimited – Distribution A

13. SUPPLEMENTARY NOTES
None

14. ABSTRACT
The objective was to integrate a mechanical test apparatus into a wind tunnel flow field capable of generating controlled multi-directional stress/strain states in flat coupons exposed to appropriate chemical, thermal, and aerodynamic shear flow environments. Displacement control enables imposition of stress/strain fields (in the flat coupons) similar to those expected in complex flight component geometries. Control and measurement of these variables and the material response in a controlled environment enables assessment of material performance for hypersonic missile and re-entry vehicle flight trajectories. Requirements for the test apparatus were developed and the apparatus was designed. Unfortunately, closure of the proposed wind tunnel facility led to increased costs and imposed a major schedule slip. The program's contract was not extended and the test apparatus was not assembled.

15. SUBJECT TERMS
High temperature material testing, supersonic flows

16. SECURITY CLASSIFICATION OF:			17. LIMITATION OF ABSTRACT	18. NUMBER OF PAGES	19a. NAME OF RESPONSIBLE PERSON
a. REPORT (U)	b. ABSTRACT (U)	c. THIS PAGE (U)		19	D. E. King
					19b. TELEPHONE NUMBER *(include area code)* 240-228-0795

Combined High Temperature Aerothermal-Structural Physical Property Testing of Ceramic Matrix Composites

AFOSR Contract: FA9550-05-1-0212

Don E. King and David G. Drewry
The Johns Hopkins University Applied Physics Laboratory
Laurel, MD, USA

Final Report
March 2008

Need

Determining the thermally degraded physical properties of advanced high temperature materials remains one of the continuing challenges facing designers of high-speed air vehicle structures. Mechanical properties of composites (ceramic or metal matrix-based) such as elastic modulus, shear modulus, and Poisson's ratio can be temperature dependent while other strength characteristics can degrade due to simultaneous exposure to high temperatures, an oxidizing environment, and structural loads. The ability to measure material characteristics in representative flight conditions will provide a unique design capability for predicting the performance of complex, multi-layer materials (including substrates and protective coatings) across a broad range of notional mission conditions. In particular, characterizing the combined effects of temperature, component geometry, aerodynamic shear, and chemical interactions on advanced aerospace materials would be extremely valuable.

Goal

Develop a test methodology to enable rapid evaluation (early in the design process) of ceramic matrix composites under combined aerothermal-structural loads and environments (see Figure 1). These conditions will simulate material performance during flight, but in a controlled laboratory environment capable of significant data collection and replicate tests.

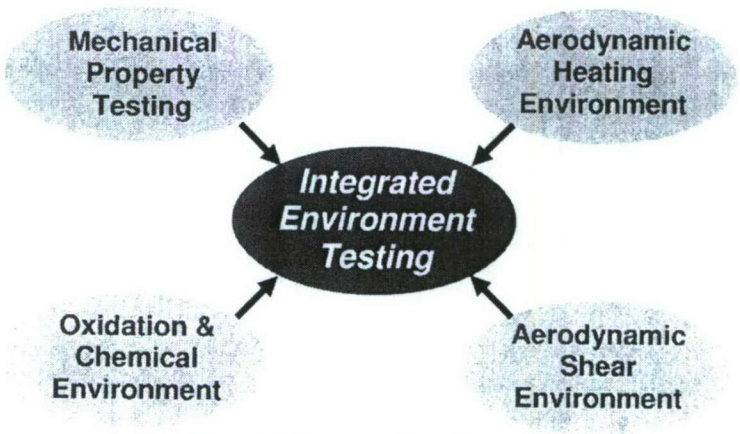

Figure 1 - Integrated testing goal.

Approach

As shown in Figure 2 below, our objective was to integrate a test apparatus (capable of producing controlled multi-directional displacements) into a wind tunnel flow field in order to generate controlled multi-directional stress/strain states in flat coupons exposed to appropriate chemical, thermal, and aerodynamic shear flow environments. Controlling these displacements enables imposition of stress/strain fields (in the flat coupons) similar to those expected in complex (i.e., non-flat) flight component geometries. In addition, manipulating the thermal, chemical, and aeroshear environments enables imposition of the anticipated atmospheric or engine conditions. Control and measurement of these variables and the material response in a controlled environment will allow prediction of material performance during flight trajectories.

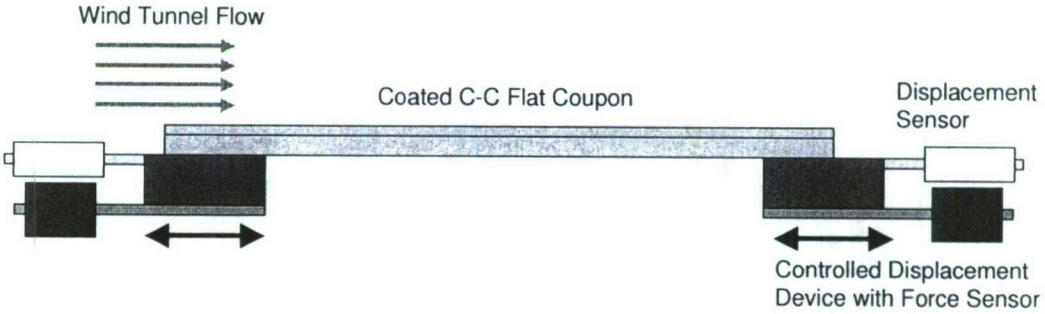

Figure 2 - Notional test apparatus design.

Discussion

When a new or existing material is proposed for a component, a series of screening tests are usually performed to validate the material's ability to survive and function in the component's operational environment. Typically, these screening tests are performed on flat coupons (due to cost and fabrication concerns) rather than on complex geometries that are more representative of the actual component. Unfortunately, flat coupons exposed only to aerodynamic loads do not necessarily experience identical (or even similar) stress and displacement fields as the actual components. Additionally, classic high temperature material property testing (e.g., a tensile test machine used in conjunction with a high temperature oven) with flat coupons does not capture degrading effects due to aerothermal and aeroshear loading: material erosion, decomposition, and chemical interaction.

The failure of flat coupon tests to adequately simulate the expected operation loads can result in scenarios where the material passes the screening tests, yet fails once it is fabricated into a multi-dimensional component and exposed to its true operational environment. For example, during combined thermal-structural loads, the developed stress-strain fields (resulting from CTE mismatches, pressure loads, bending loads, etc.) in the material can lead to local micro-cracking of surface coatings and in worst cases, spallation of protective coatings from the substrate. The sensitivity of the coating response can also be influenced by thermal loading rates (thermal shock and thermal cycling), aerodynamic shear forces, duration of exposure, and gas composition.

Initial studies indicated that the stress-strain fields of curved flight components (which may experience hoop stresses in addition to axial stresses) could be simulated via

controlled displacements applied to flat coupons. When coupons undergoing such displacements are simultaneously exposed to aerothermal and aeroshear loads in an oxidizing environment and while under imposed mechanical displacements, the material behavior during flight conditions can be more accurately assessed. Such a test capability would be useful across the entire life of a material system (see Figure 3). During preliminary design, tests can be performed to screen and downselect candidate materials. Later in the design process, higher fidelity performance data can be obtained by applying time-varying stress-strain fields and aerothermal environments to simulate the anticipated flight scenario. Finally, production hardware can be periodically evaluated via witness coupon testing.

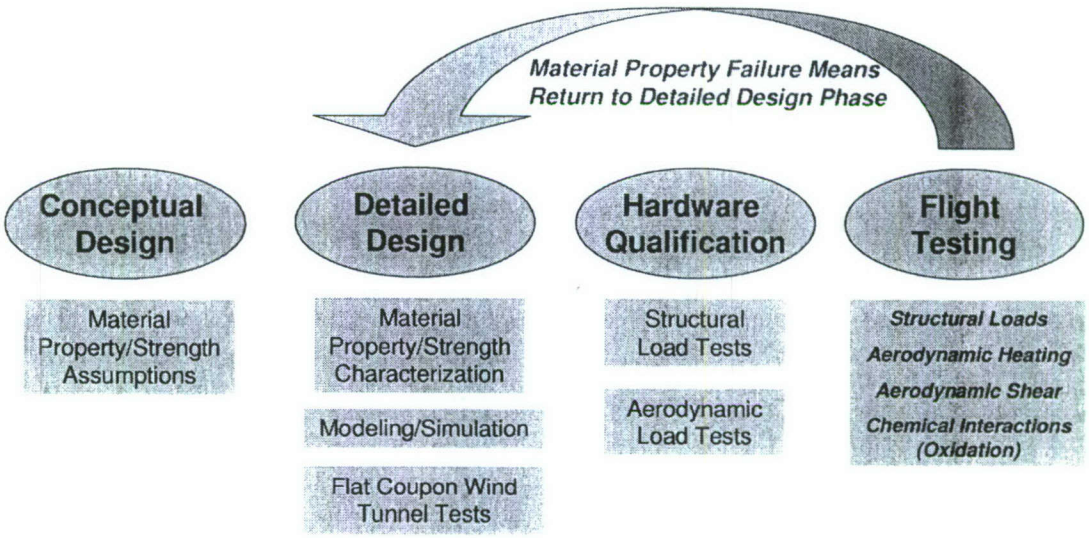

Method of Simulating Flight Environments During Early Material Testing Could Predict Design Problems before Flight Testing

Figure 3 - Use of test capability across design process.

Status

During the **first year** of the program (beginning with receipt of funds in April 2005), requirement studies were conducted to capture the thermal, chemical, aerodynamic, and structural loads that the materials used in aerospace vehicle would be exposed to during flight (see Figure 4 for typical examples). These flight environment conditions were then mapped against wind tunnel capabilities of Cell 4 at JHU/APL's Avery Advanced Technology Development Laboratory (AATDL). Thus, the required wind tunnel operating conditions were correlated against a wide range of engine and airframe operational environments.

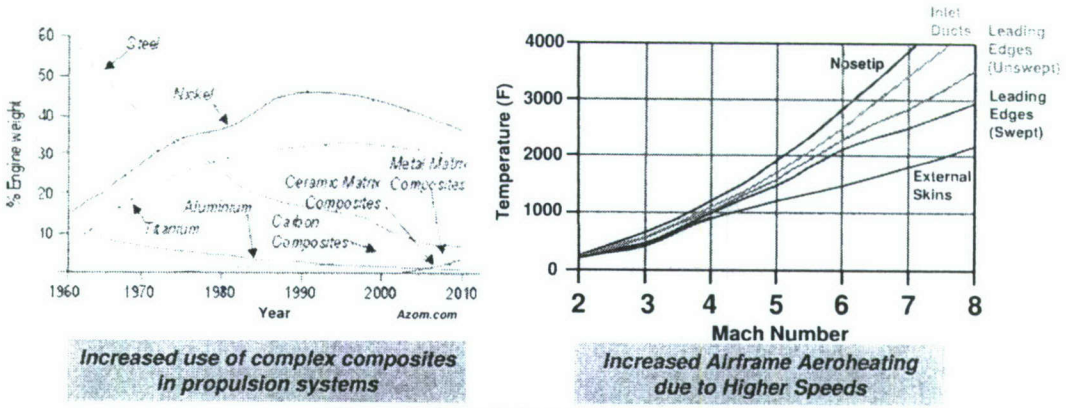

Figure 4 - Trends in aerospace hardware.

Structural load requirements were also collected during this phase. The required displacements necessary for the flat coupons to simulate internal stress fields of curved vehicle components (see Figure 5 and Figure 6) were derived for a number of applications (e.g., pressurized combustion chambers, high-speed external flow, etc.). Mechanical loads requirements were identified for the following flight scenarios: (i) prior to aerothermal loads (simulating captive carry and pre-launch exposure); (ii) during sustained time-varying aerothermal heating (simulating flight loads); and (iii) post heating (simulating terminal maneuvers).

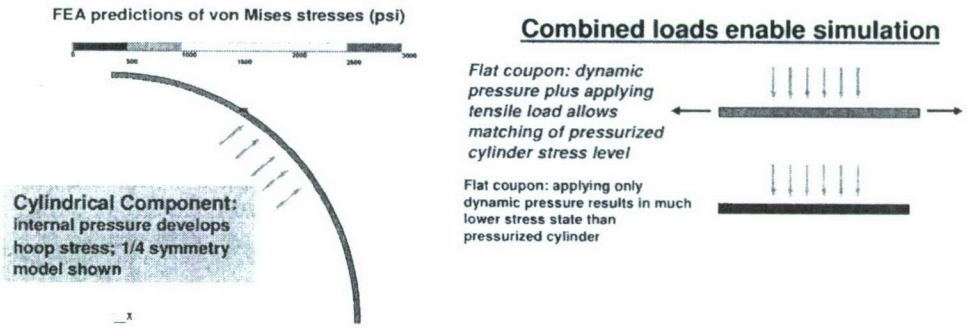

Figure 5 - Capturing geometry effects with flat coupon.

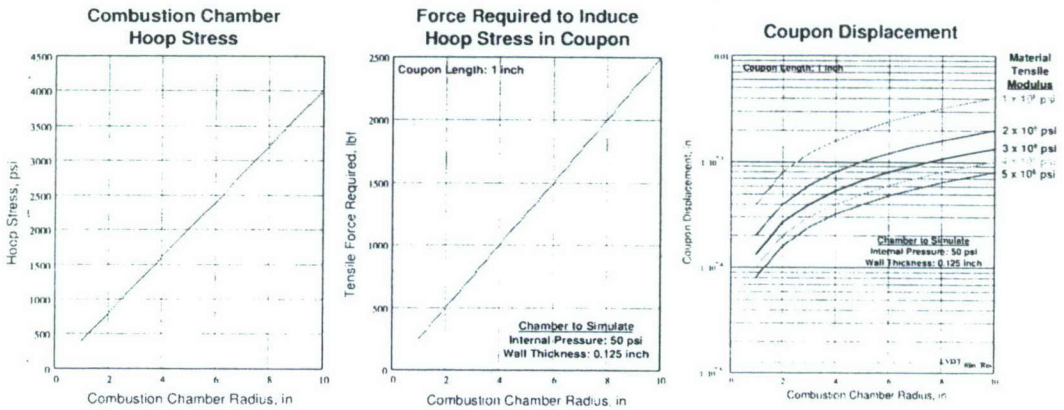

Figure 6 - Example of flat coupon displacement required for simulating curved flight component.

Controlling the aerothermal, aerodynamic shear, and oxidation environments, along with the test coupon's mechanical displacement would enable simulation of flight environments as shown in Figure 7.

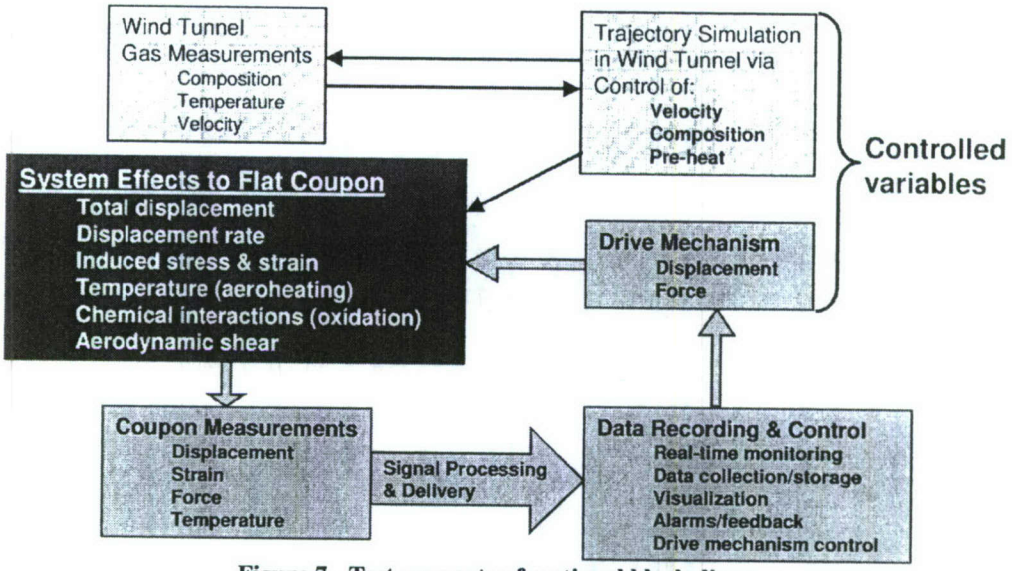

Figure 7 - Test apparatus functional block diagram.

Coupon sizing studies were performed. The essential displacement measurement resolution was trade-off against available displacement methods (e.g., controlled displacement motor, geared screw mechanism, etc.) as a function of the required induced stress-strain fields. In addition, the coupon size necessary to minimize edge effects was also examined. The results indicated that the design was feasible using readily available commercial-off-the-shelf (COTS) components as shown in Figure 8.

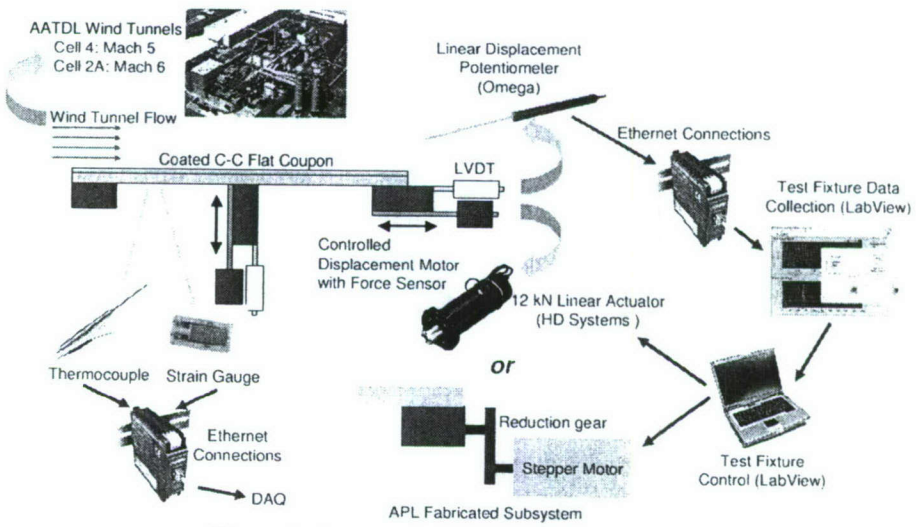

Figure 8 - Initial test fixture component design.

Unfortunately, in our **second year** we encountered issues that significantly affected our program plan and schedule. After a period of internal debate and study, JHU/APL

management decided to close AATDL and its associated wind tunnels. This decision was made for the same reasons that many wind tunnels have been closed (or mothballed) in recent years - the overhead costs associated with such facilities became excessive. Attempts were made to preserve some capabilities by transferring equipment to the main JHU campus, but these also proved to be cost-prohibitive, resulting in all the AATDL wind tunnel facilities being either sold off or demolished (see Figure 9). The end result is that we lost access to not only the wind tunnel proposed for test apparatus integration, but also the support equipment we planned to use in fabricating the test apparatus. This support equipment included computers, sensors, data acquisition systems, and hardware. In addition, the tunnel support personnel who were experienced in fabricating and operating tunnel test hardware were dispersed throughout APL and given other responsibilities. As such, access to their abilities and talents was reduced.

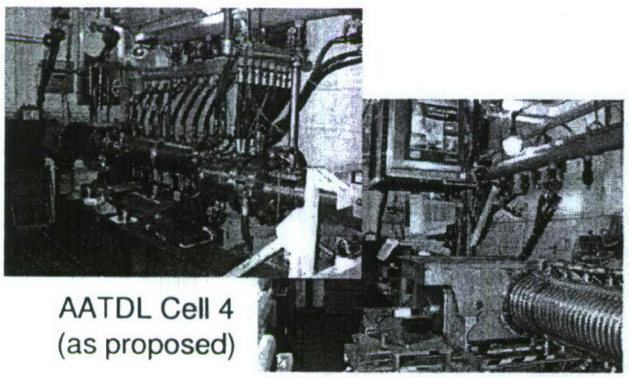

AATDL Cell 4
(as proposed)

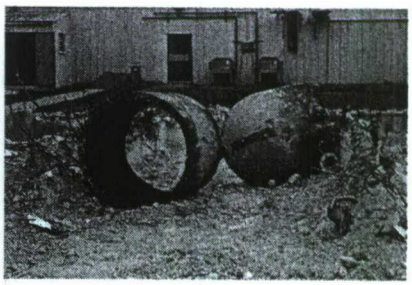

AATDL Cell 4
(today)

Figure 9 - Demolition of AATDL facilities.

During the period of uncertainty leading up to the closure decision, the principal investigators decided to reduce the program fund burn rate for two primary reasons:

1. *Avoiding significant redesign effort.* Since the test apparatus must be sized to fit into a wind tunnel, there was concern that continuing the baseline design effort (based on the AATDL Cell 4 internal diameter) could restrict the apparatus' ability to be integrated into smaller wind tunnels. A survey of potential wind tunnels needed to be conducted to determine the maximum allowable dimensions of the test apparatus.
2. *Preservation of funds to support future tunnel integration efforts.* Closure of the AATDL obviously means that another wind tunnel (or tunnels) will be required to complete the program. Until options for the new wind tunnel(s) are identified, the costs associated with future integration/testing are unknown. Since the original costing assumed use of AATDL, no travel was budgeted, but travel will now be required. Equipment costs will be higher, as many items that could have been used in the test apparatus (such as screw gears, Ethernet wiring, support structures, etc.) have now been discarded. It is also likely that use of any new tunnel will cost more than that originally budgeted for the APL facilities. Until cost data for other tunnels could be obtained, it was deemed prudent to preserve funds.

In our **third year**, technical activities targeted the following issues:

- Identification of other wind tunnel facilities to assess their potential to serve as an integration test bed.
- Coupon design studies focused on minimizing edge effects and ensuring that the appropriate stress and strain fields are developed in the center of the test coupon.
- Characterization and selection of displacement measurement approach.
- Design of a "generic" test apparatus which can be deployed to various wind tunnel facilities.
- The paper, "Combined High Temperature Aerothermal-Structural Physical Property Testing of Ceramic Matrix Composites," was presented at the *14th AIAA/AHI Space Planes and Hypersonic Systems and Technologies Conference* in Canberra, Australia[1]. An update to this paper was accepted for the AIAA 2008 hypersonics conference in Dayton, OH. (Due to the denial of our requested FY08 no-cost contract extension, this paper will have to be withdrawn).

Wind tunnel facilities

Using recent data[2,3], a survey of other wind tunnel facilities capabilities, relative cost, and test area dimensions was conducted. Since development of oxidation and thermal profiles through the test coupon will require test times of several (tens of) seconds, tunnels (such as shock tubes) only capable of generating short test times were not considered. Several potential opportunities were identified as shown in the table below:

Potential Wind Tunnels for Test Apparatus Integration						
Facility	Capabilities				Relative Testing Cost	Test Area Limits
	Aerothermal	Aeroshear	"Altitude"	Oxidation		
AFRL - LHMEL	High (via laser)	Low	Low to High	Yes	Low	< 3 in wide
AEDC	High	High	High	Yes	Very High	25 in to 50 in
NASA - Langley Res Ctr	High	High	High	Yes	High	6 in to 120 in
NASA – Marshall HGF	High	High	Low to High	Yes	Medium	14 in to 32 in
CAES - ONR (proposed)	High	TBD	TBD	Yes	Low	TBD

A major requirement for any wind tunnel used for materials research is low cost per test. This is because a material characterization test program typically requires numerous test runs to evaluate different material formulations. Two tunnels that meet the low cost requirement are the Air Force Research Laboratory's Laser Hardened Materials Evaluation Laboratory (LHMEL) and the tunnel being considered for development by Custom Analytical Engineering Systems for the Office of Naval Research (CAES-ONR). While tunnels at other facilities, Arnold Engineering Development Center (AEDC) and NASA-Langley, would enable simulation of operational conditions, their testing costs are higher which would result in fewer tests being conducted, thus limiting their overall effectiveness in any material development and evaluation program. NASA-Marshall's Hot Gas Facility offers simulation of operation conditions at a lower price than the AEDC and NASA-Langley tunnels.

AFRL's LHMEL's wind tunnel is attractive due to its relatively low cost per test. While LHMEL is capable of generating high temperatures in the test coupon, these

temperatures are the result of laser energy, not aeroheating. Supersonic flow (to a maximum of Mach 2.3) in an oxidizing environment can be achieved at pressures less than one atmosphere but with low levels of aeroshear. The tunnel also has a very restrictive area for integrating the test apparatus, indicating that some kind of adapter section would be required to mount the test apparatus while still aiming and controlling the airflow over the test coupon.

The AEDC, NASA-Langley, and NASA-Marshall HGF tunnels can provide challenging aerothermal, aeroshear, and oxidation environments for testing and also possess sufficient size for easy mounting of the test apparatus in their wind tunnels. However, as previously mentioned, the cost of testing at the AEDC and NASA-Langley facilities will preclude performing in-depth experimental studies of material properties. Material testing at these tunnels would more likely be focused on validating the function of a final material formulation (in an anticipated operating environment) instead of developing or optimizing the material formulation via experimental trials.

In addition to the previously mentioned favorable test conditions, the NASA-Marshall HGF offers a relatively large test area and reasonable test costs. This combination of features makes the HGF very appealing for material characterization tests using our test apparatus.

Besides the benefit of low testing costs, the CAES-ONR tunnel also appears very interesting for other reasons. This tunnel is planned for high-temperature material development activities supporting ONR's Electromagnetic Railgun (EMRG) projectile. The facility will thus be optimized to rapidly conduct material characterization tests at low cost while still achieving test conditions that will simulate stressing operational environments. As a member of the EMRG team, APL is currently assisting with the design of this tunnel and as such, is able to make suggestions to enable future integration of our test apparatus.

Test coupon studies

As originally conceived, the test rig would have applied only uniaxial tension or compression loads. Our investigations have convinced us of the need to induce biaxial stress fields in order to better characterize the performance of composite laminates, since these laminates usually experience more than uniaxial stresses in structures of practical interest[4]. Even when uniaxial loads are applied, the complex structure of laminates can result in three dimensional stress states in fabricated structures[5]. Replication of operational stress and strain states is necessary for proper understanding of coating and substrate responses including:

- Substrate failure:
    - fiber pull-out
    - delamination
    - matrix failure
    - oxidation (coupled to coating failure)
- Coating failure:
    - crazing/cracking
    - delamination/spallation

Data collected under biaxial loading can also be used in micromechanics-based multicontinuum theory (MCT) to obtain better predictions of composite failure than previous failure theory predictions (made using data from uniaxial load cases) [6,7,8].

The biaxial test coupons will use a cruciform design similar to ones shown below that have proven effective in biaxial testing of composite laminates[7,9,10]. As shown in Figure 10, these proven designs feature a thinned center section with rounded edges to insure that the maximum stresses are developed in the portion of the test coupon under biaxial loading and not along the cruciform's arms (which only experience uniaxial loads). As shown in Figure 11, the center portion of these cruciforms is available for instrumentation with strain gauges and thermocouples.

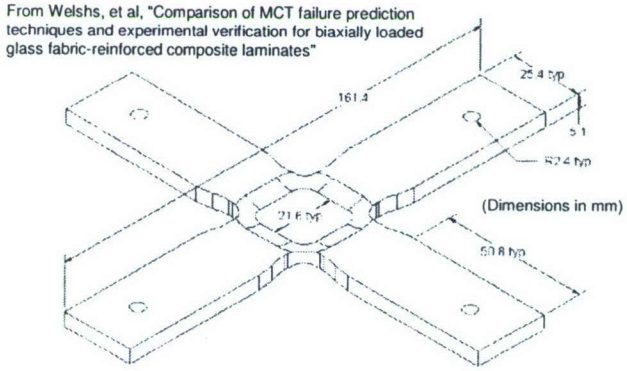

Figure 10 - Typical cruciform test coupon for biaxial load tests.

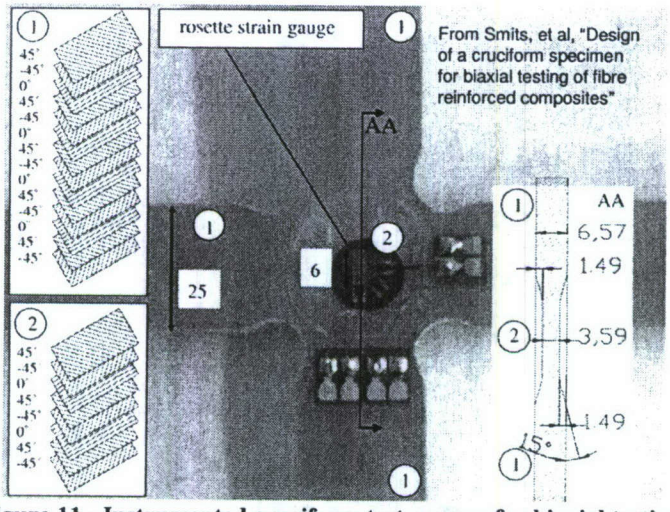

Figure 11 - Instrumented cruciform test coupon for biaxial testing.

Our coupon design differed from those shown in that the upper surface of our cruciform (that is, the surface exposed to the wind tunnel flow) must be flat for undisturbed airflow (necessary to develop the desired boundary layer conditions) across the coated surface. In addition, the mounting details at the end of the upstream arm also differ, since a clamp cannot protrude into the airflow upstream of the center test portion of the cruciform. A clamp would, however, be employed on the downstream arm. The transverse arms (in most wind tunnel flow conditions) would also be able to utilize

clamps, since the airflow disturbance in most conditions will not affect the flow over the cruciform's center test portion.

We have conducted finite element simulation of these types of test coupons (see Figure 12Figure 13, and Figure 14). A carbon-carbon (C-C) composite cruciform coated with a thin layer of silicon carbide (SiC) was placed under biaxial tension, biaxial tension/compression, and uniaxial tension and compression loads. As shown below, the maximum stresses were located in the center test region of the cruciform*. Additional finite element studies are being conducted to: (i) confirm that our coupon design (with a flat upper surface) maintains the maximum stresses in the center region and (ii) minimize stresses in the pin regions (to prevent pin pull-through).

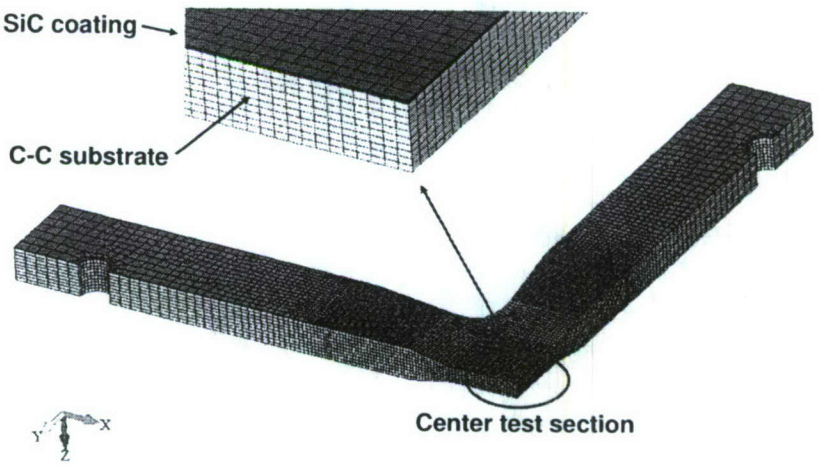

Figure 12 – Quarter symmetry view of finite element model of SiC coated C-C cruciform.

* Blue = low and red = high stress levels. Tensile stress is positive and compressive stress is negative.

Figure 13 - Maximum stresses under biaxial loads (quarter symmetry view).

Figure 14 - Maximum stresses under uniaxial loads (quarter symmetry view).

Displacement measurement approach

Displacement and strain measurements will initially be made via strain gauges. Stress fields will be generated using the strain field measurements and the elastic modulii of the composite's components. Strain in the test portion of the material coupon will be measured via strain gauges attached to the unexposed side of the test coupon (for obvious reasons, the gauges cannot be mounted on the side of the coupon exposed to the wind tunnel airflow). Care will be taken in the mounting procedure to insure that both the strain gauges and adhesive used will be capable of surviving the test coupon's anticipated high temperatures.

The potential for measuring the developed strain field via optical measurements (using laser speckle[11,12,13,14] or photogrammetry[15] techniques) was also investigated during the third year. As shown in Figure 15, these techniques illuminate surface features (with either broadband light or a laser), take a sequence of images while the structure is under test, then numerically track and analyze feature movement to calculate the displacement field. The displacement field is then normalized to generate the strain field.

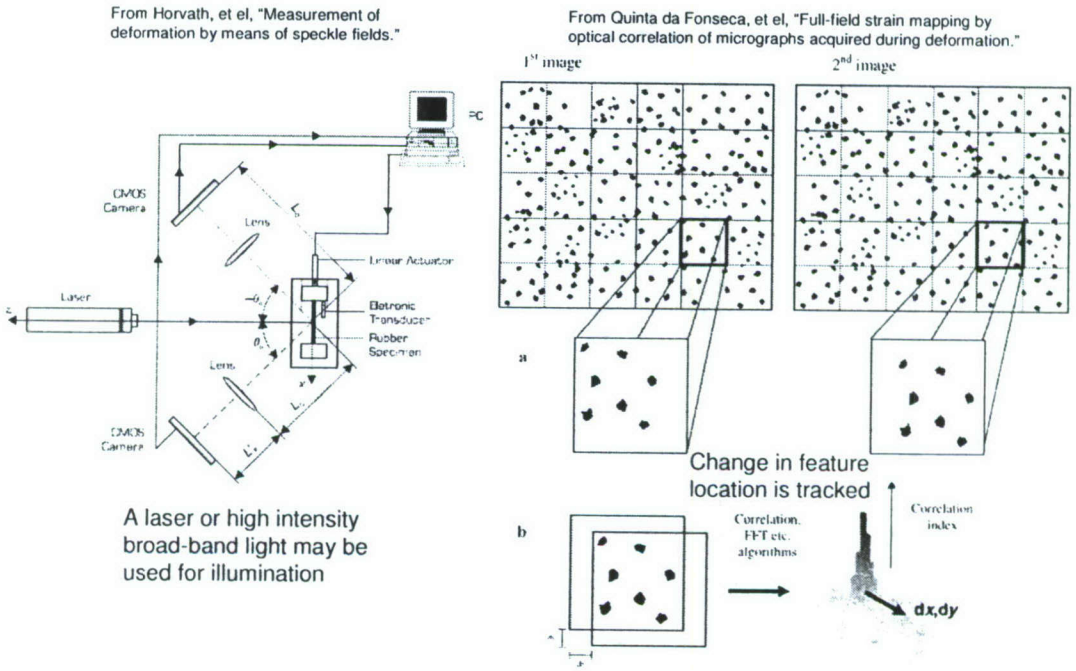

Figure 15 - Basis for non-contact optical displacement measurement.

Optical displacement measurements exploit non-contact techniques that permit in situ measurement of the strains developed in the exposed hot surface of a test coupon[16,17]. Such non-contact and full field techniques could overcome two limitations imposed by the use of strain gauges: the requirement to use high temperature mounting methods and the collection of local (versus global) strain data[18].

Knowledge of the global strain field on the exposed surface provides three major advantages: (i) confirmation that the maximum strains were in the center test portion of

the coupon and not in the coupon's arms, (ii) accurate mapping of developed strains to coating failure locations, and (iii) the ability to predict coupon material properties via an inverse solution technique using numerical models. The first advantage validates the test. The second advantage yields insight into the relationship between surface strain and coating failure. The third advantage enables characterization of material properties (such as orthotropic tensile, compressive, and shear modulii and Poisson's ratio) during anticipated operational loads and environments[19]. As shown in Figure 16, an iterative approach is then used to adjust the material properties until the difference between the numerical and experimental strains is minimized.

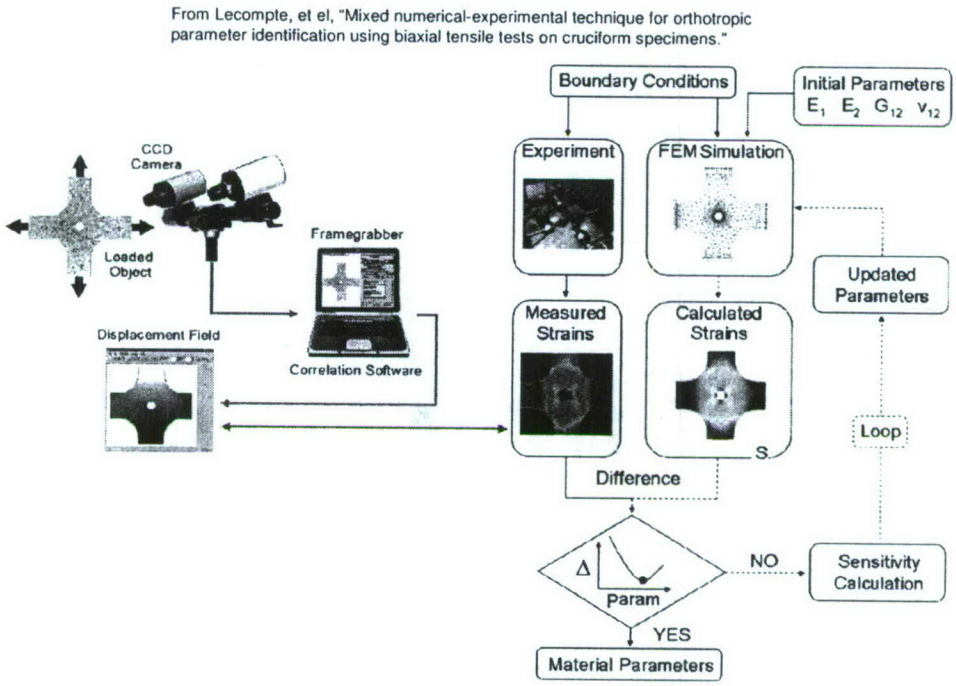

Figure 16 - Approach to determine material properties from biaxially leaded cruciform experiment.

The difficultly in using these highly desirable optical displacement measurement methods is obtaining accurate images through the dynamic boundary layer above the test coupon[20]. As shown in Figure 17, density fluctuations within the boundary layer result in high frequency temporal and spatial fluctuations in the gas index of refraction[21]. The consequences of such rapid changes in refractive index are twofold: (i) beam wander and (ii) beam spread[22]. In the case of the latter, the intensity of the signal at the sensor would decrease, thus decreasing the signal-to-noise ratio at the sensor. In the case of the former, the apparent location of the speckle or surface feature would not be accurate (as shown below). Thus, the displacement calculation (which is based on tracking changes in the speckle or feature location) would be in error. When using laser speckle imaging techniques, these effects would be further amplified. The laser beam would be affected both on its way through the boundary layer to the surface, and then (after the beam's reflection) on its way from the surface back to the sensor.

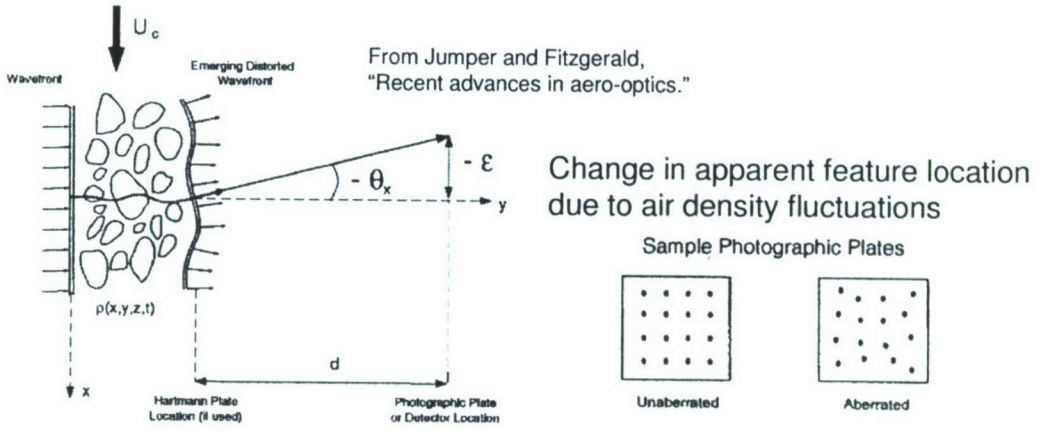

Figure 17 - Aero-optic problem of imaging through a boundary layer.

Unfortunately, while great progress has been recently been made in solving the aero-optic problem of imaging through boundary layers[23], these techniques do not appear to be "turnkey" enough for our use. Indeed, proper adaptation, implementation, and validation of typical optical wavefront reconstruction methods in our application would constitute another entire research project involving fabrication of state-of-the-art sensors and construction of imaging processing algorithms. Thus, attempting to optically measure displacements on the coupon's exposed upper surface was deemed not practical at this time.

Since there are no aero-optical imaging concerns with the coupon's lower (protected) surface, the option to conduct optical measurement of this surface's displacement will continue to be carried forward. This will be done by designing the test apparatus with an opening beneath the center of the test coupon thus allowing real-time digital imaging (using currently available commercial systems) of the lower surface to be conducted during a test. While such an approach is not optimum, using the experimental strain results from the lower coupon surface will still enable material property characterization using the previously outlined iterative approach. Use of these properties in the finite-element model will enable prediction of upper surface and through-thickness strains and stresses.

Thermal measurements

Temperature measurements of the test coupon will be made via thermocouple(s) attached to its lower side. In addition, standard tunnel instrumentation should allow for non-contact infrared temperature measurement and/or imaging of the coupon's upper surface during testing (provided the emissivity of the surface as a function of temperature is known or characterized prior to wind tunnel testing). Even with degradation due to aero-optical effects, real time thermal imaging movies should provide valuable data regarding the coupon's exposed surface interaction with the high-speed, oxidizing airstream. In particular, changes in surface emissivity due to coating oxidation or aeroshear "wiping off" of a partially melted coating will be measurable. When coupled with surface temperature and wind tunnel airflow data, the emissivity change will provide information on the design limits of the protective coating.

As previously noted, the test apparatus is designed to allow real-time imaging of the lower surface of the coupon during a test. Thus, similar non-contact thermal measurements methods can be used to collect the same thermal data as on the upper (exposed) side. Coupling this data with a finite element model (using temperature dependent thermal properties) will provide prediction of upper surface and through-thickness temperatures. Coupled with independent measurement of the upper surface temperature, the inverse problem can be solved to derive temperature-dependent thermal material properties (conductivity, diffusivity, and specific heat) from the finite element model.

Test apparatus

The test apparatus design has been refined and components are under order. The schematic in Figure 18 shows the displacement test unit's primary components and operation. A pneumatic-hydraulic system was selected to provide sufficient force and control to induce controlled strain levels in the test cruciform. The test apparatus shown below is capable of applying uniaxial or biaxial tension loads to the cruciform. Additional hydraulic cylinders may be attached to the edges of the test apparatus to apply compression loads. Thus, the test apparatus will be capable of spanning the entire range of loads (tension/tension, tension/compression, and compression/compression) necessary for evaluating the composite's performance against current composite failure theories[24].

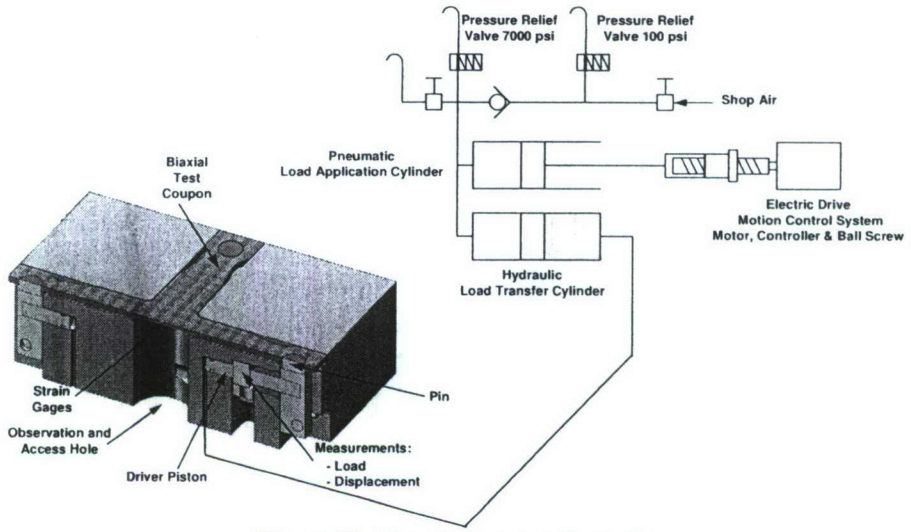

Figure 18 - Test apparatus schematic.

The requirements of (i) undisturbed airflow over the center portion of the test coupon and (ii) maintaining a small test apparatus footprint necessitate using an "out-of-plane" design for inducing strain. To meet these requirements, the displacement cylinders must be mounted underneath the test cruciform.

To ensure that failure occurs in the center test portion of the cruciform, the uniaxial portions of the cruciform will have a larger cross-sectional area than the center test

portion. The combination of final pin shape (circular, elliptical, or rectangular) and cruciform leg thickness will be selected in order to ensure that pin "pull-through" does not occur.

The width of the test cruciform legs and the width of the raceways in the upper surface of the test apparatus are sufficiently different that cruciform leg growth (due to the applied load and thermal expansion) will not cause the cruciform leg to contact the sidewalls of the raceway during a test. The dimensions and tolerances of the test apparatus and cruciform specimen will be designed to minimize effects due to the thermal expansion mismatch between the metal test apparatus and the ceramic cruciform. Our experience indicates that the thermal mass and thermal diffusivity of the test apparatus, combined with the limited exposure time, will enable use of an uncooled test apparatus. If future tests require cooling the test apparatus, either a series of "L" shaped coolant channels could be drilled into the lower portion of the test structure or an external cooling jacket could be used.

Data collection and displacement control will be via a laptop computer running LabView software. Displacement of the various cylinders will be measured as well as coupon strain (via strain gauges) and coupon temperature (via thermocouples or non-contact means). As shown in Figure 19, a simple feedback loop will be used to drive cylinder displacement until the desired coupon strain is achieved. Real time information of the displacements, strains, temperatures, and calculated stresses will be displayed. Additional data such as non-contact strain fields will be recorded via separate stand-alone systems. Wind tunnel conditions (velocity, pressure, temperature, species, etc.) will be collected by the tunnel data acquisition system. A common timestamp will be used to synchronize the separate data collection sources for post-run processing.

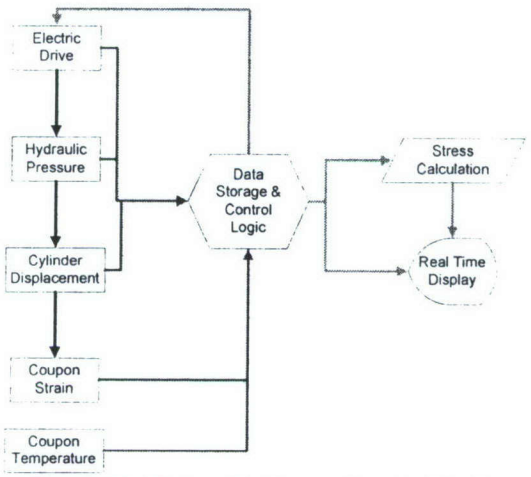

Figure 19 - Data collection and control logic.

FY2008 Activities

Due to a combination of (i) receiving our first year funds approximately six months late and (ii) the previously mentioned spending slow down in our second year, approximately $100K of funds remained at the end of December 2007. We formally

requested a no-cost contract extension through the end of FY2008 (30 September 2008) in order to complete the following activities:

- Use FEA to finalize test cruciform dimensions and shape
- Fabricate and instrument the test apparatus
- Complete the LabView control program

The requested no-cost contract extension was denied, and all remaining funds will be returned to AFOSR.

Acknowledgment/Disclaimer

This work was sponsored by the Air Force Office of Scientific Research, USAF, under grant/contract number FA9550-05-1-0212. The views and conclusions contained herein are those of the authors and should not be interpreted as necessarily representing the official policies or endorsements, either expressed or implied, of the Air Force Office of Scientific Research or the U.S. Government.

Publications

King, D. E., D. G. Drewry, and M. G. Thompson, "Combined High Temperature Aerothermal-Structural Physical Property Testing of Ceramic Matrix Composites," presented at the *14th AIAA/AHI Space Planes and Hypersonic Systems and Technologies Conference*, November 2006.

Personnel Supported or Associated

Mr. Don E. King, P.E.	Senior Professional Staff, Global Engagement Department
Mr. David G. Drewry	Principal Professional Staff, Global Engagement Department
Mr. Michael W. Thompson	Senior Professional Staff, Global Engagement Department
Mr. Tom Wolf	Senior Professional Staff, Global Engagement Department
Mr. Martin Annett	Senior Professional Staff National Security Technology Department

References

[1] King, D. E., D. G. Drewry, and M. G. Thompson, "Combined High Temperature Aerothermal-Structural Physical Property Testing of Ceramic Matrix Composites," presented at the *14th AIAA/AHI Space Planes and Hypersonic Systems and Technologies Conference*, November 2006.

[2] Anton, P. S., et al, *Wind Tunnel and Propulsion Test Facilities: An Assessment of NASA's Capabilities to Serve the Nation*, RAND Corporation, 2004.

[3] Anton, P. S., et al, *Wind Tunnel and Propulsion Test Facilities: Supporting Analyses to an Assessment of NASA's Capabilities to Serve the Nation*, RAND Corporation, 2004.

[4] Lin, W.-P. and H.-T. Hu, "Parametric Study on the Failure of Fiber-reinforced Composite Laminates under Biaxial Tensile Load," *Journal of Composite Materials*, 36(12), pp. 1481-1503, 2002.

[5] Welsh, J. S., et al, "2-D Biaxial Testing and Failure Predictions of IM7/977-2 Carbon/Epoxy Quasi-isotropic Laminates, *Composite Structures*, 75, pp. 60-66, 2006.

[6] Mayes, J. S., and A. C. Hansen, "Composite Laminate Failure Analysis Using Multicontinuum Theory," *Composites Science and Technology*, 64, pp. 379-394, 2004.

[7] Welsh, J. S., et al, "Comparison of MCT Failure Prediction Techniques and Experimental Verification for Biaxially Loaded Glass Fabric-reinforced Composite Laminates, *Journal of Composite Materials*, 38(24), pp. 2165-2181, 2004.

[8] Mayes, J. S., and A. C. Hansen, "A comparison of multicontinuum theory based failure simulation with experimental results," *Composites Science and Technology*, 64, pp. 517-527, 2004.

[9] Welsh, J. S. and D. F. Adams, "An Experimental Investigation of the Biaxial Strength of IM6/3501-6 Carbon/Epoxy Cross-Ply Laminates Using Cruciform Specimens," *Composites, Part A*, 33, pp. 829-839, 2002.

[10] A. Smits, et al, "Design of a Cruciform Specimen for Biaxial Testing of Fibre Reinforced Composite Laminates," *Composites Science and Technology*, 66, pp. 964-975, 2006

[11] Yamaguchi, I., "A Laser-speckle Strain Gauge," *Journal of Physics E: Scientific Instruments*, 14, pp. 1270-1273, 1981.

[12] Yamaguchi, I., et al, "Stabilized and Accelerated Speckle Strain Gauge," *Optical Engineering*, 32(3), pp. 618-625, 1993.

[13] Tanabe, Y., et al, "In Situ Speckle Observation of Tyrano/BMAS Composites in Shear Strength Measurements," *Composites: Part B*, 34, pp. 399-403, 2003.

[14] Horvath, P., et al, "Measurement of Deformation by Means of Correlation of Speckle Fields," *Experimental Mechanics*, 46, pp. 713-723, 2006.

[15] Tyson, J. and T. Schmidt, "Advanced Photogrammetry for Robust Deformation and Strain Measurement," *Proceedings of SEM 2002 Annual Conference*, Milwaukee, WI, June 2002.

[16] Anwander, M., et al, "Noncontacting Strain Measurements at High Temperatures by the Digital Laser Speckle Technique," *Experimental Mechanics*, 40(1), pp. 98-105, 2000.

[17] Uchimura, H., et al, "Measurement of Biaxial Displacement by a Speckle Correlation Method at High Temperature," *Journal of the American Ceramic Society*, 78(12), pp. 3273-3276, 1995.

[18] Quinta da Fonseca, J. et al, "Full-field Strain Mapping by Optical Correlation of Micrographs Acquired During Deformation," *Journal of Microscopy*, 218, pp. 9-21, 2005.

[19] Lecompte, D., et al, "Mixed Numerical-experimental Technique for Orthotropic Parameter Identification using Biaxial Tensile Tests on Cruciform Specimens," *International Journal of Solids and Structures*, 44, pp. 1643-1656, 2007.

[20] Sutton, G. W., "Effect of Turbulent Fluctuations in an Optically Active Fluid Medium," *AIAA Journal*, 7(9), pp. 1737-1743, 1969.

[21] Wyckham, C. M., et al, "Characterization of Optical Wavefront Distortions due to a Boundary Layer at Hypersonic Speeds," *34th AIAA Plasmadynamics and Lasers Conference*, AIAA 2003-4308, June 2003.

[22] Sutton, G. W., "Aero-optical Foundation and Applications," *AIAA Journal*, 23(10), pp. 1525-1537, 1985.

[23] Jumper, E. J. and E. J. Fitzgerald, "Recent Advances in Aero-optics," *Progress in Aerospace Sciences*, 37, pp. 299-339, 2001.

[24] Hinton, M. J., et al, "Evaluation of Failure Prediction in Composite Laminates: Background to 'Part B' of the Exercise," *Composites Science and Technology*, 62, pp. 1481-1488, 2002.